

Structure and properties of two-phase $\text{Cd}_x\text{Pb}_{1-x}\text{S}/\text{CdS}$ films obtained by chemical deposition from the ethylenediamine-citrate system

© A.D. Selyanina¹, L.N. Maskaeva^{1,2}, V.I. Voronin³, I.O. Selyanin⁴, I.A. Anokhina⁵, V.F. Markov^{1,2}

¹ Ural Federal University after the first President of Russia B.N. Yeltsin, 620002 Yekaterinburg, Russia

² Ural Institute of State Fire Service of EMERCOM of Russia, 620062 Yekaterinburg, Russia

³ M.N. Mikheev Institute of Metal Physics, Ural Branch, Russian Academy of Sciences, 620108 Yekaterinburg, Russia

⁴ Institute of Solid State Chemistry, Russian Academy of Sciences, Ural Branch, 620990 Yekaterinburg, Russia

⁵ Institute of High-Temperature Electrochemistry, Ural Branch, Russian Academy of Sciences, 620137 Yekaterinburg, Russia

E-mail: n-kutyavina@mail.ru

Received December 8, 2021

Revised December 14, 2021

Accepted December 14, 2021

Polycrystalline films of $\text{Cd}_x\text{Pb}_{1-x}\text{S}$ ($0 \leq x \leq 0.05$) substitutional solid solutions with a cubic structure $B1$ ($Fm\bar{3}m$ space group) containing amorphous cadmium sulfide were obtained by chemical bath deposition. Upon reaching a critical concentration of the cadmium salt in the reactor, the films consisted of substitutional solid solution and cubic CdS with the $B3$ structure ($F4\bar{3}m$ space group). Scanning electron microscopy established the morphological features associated with the secondary nucleation and formation of the cadmium sulfide phase. The structural characteristics of the films have been calculated by a full-profile analysis of X-ray diffraction patterns. We have revealed the correlation between phase and elemental composition of $\text{Cd}_x\text{Pb}_{1-x}\text{S}/\text{CdS}$ films with their voltage and current photosensitivity. Based on the received data, we have assumed the role of the individual CdS phase for the photoconductivity mechanism of $\text{Cd}_x\text{Pb}_{1-x}\text{S}$ solid solutions.

Keywords: chemical bath deposition, thin films, solid solutions, cadmium sulfide, photosensitivity, current-voltage characteristics.

DOI: 10.21883/SC.2022.04.53234.9783

1. Introduction

Ternary compounds in the CdS–PbS system are one of the classic materials of optoelectronics in the visible and near-infrared spectral ranges ($0.4\text{--}3\ \mu\text{m}$) [1,2] with a variable band gap from narrow-gap PbS $0.4\ \text{eV}$ up to wide-gap CdS $2.42\ \text{eV}$ [3,4]. Despite the great progress in the study of thin films of substitutional solid solutions (SSS) $\text{Cd}_x\text{Pb}_{1-x}\text{S}$ [1–4] and quantum-dimensional heterostructures based on them [5–7], there is still no complete understanding of the relationship between the photoelectric properties of these materials and their morphology and composition.

The preparation method often has a great influence on the thin film coatings composition and properties. The literature describes both physical and chemical methods for obtaining $\text{Cd}_x\text{Pb}_{1-x}\text{S}$ solid solutions, in particular, vacuum evaporation [8] and spray pyrolysis [9,10]. However, researchers prefer the hydrochemical precipitation method [1–4,11–16], as it does not require sophisticated equipment and is easy to implement. An undeniable advantage of the hydrochemical method is also the ability to control *in situ* the morphology, composition, structure and, consequently, the electrical and functional properties

of $\text{Cd}_x\text{Pb}_{1-x}\text{S}$ by changing the deposition conditions (pH, temperature, process duration) and concentrations of the reaction mixture components [12–16]. It is known [17], that a complexing agent (ligand) regulates the rate of a solid phase formation by supplying free Me^{2+} ions to the reaction region during the dissociation of complexes, being the most effective means of influencing the synthesized layers properties, so the researchers are experimenting with the selection of ligands. For an alkaline environment, triethanolamine ($\text{C}_6\text{H}_{15}\text{NO}_3$), an aqueous solution of ammonia (NH_4OH), sodium citrate ($\text{Na}_3\text{C}_6\text{H}_5\text{O}_7$), ethylenediamine ($(\text{NH}_3)_2(\text{CH}_2)_2$) or a combination of these substances are often selected.

An analysis of the literature shows, that the use of certain complexing agents or their combination does not always have a positive effect on the $\text{Cd}_x\text{Pb}_{1-x}\text{S}$ films composition and properties. In the study [16], film samples were obtained from baths containing triethanolamine, the highest photocurrent value ($25\ \mu\text{A}$) for which was observed in the wavelength range $500\text{--}800\ \text{nm}$, that indicates a high content of cadmium sulfide in them.

CdPbS (5% Pb) and CdPbS (20% Pb) films obtained from a reaction mixture containing ammonia [18] as a ligand, demonstrate an increase in current upon illumination by 8

and 13 times respectively, as well as a decrease in the conductivity and an increase in the activation energy of layers conductivity with an increase in cadmium in the composition of CdPbS [19] films. Pentia et al. obtained CdPbS layers using EDTA (ethylenediaminetetraacetic acid) and ammonia [2] as ligands. After heat treatment at 373 K, the resulting samples had a maximum spectral sensitivity in the range of 1800–1900 nm, however, the highest signal values were recorded, when the layers were cooled below 100 K. Note, that in the above publications, the authors do not give the true composition of the solid solution, but indicate only the elemental composition. Freshly deposited films of Cd_xPb_{1-x}S solid solutions obtained by chemical deposition from a reaction mixture containing ammonia for cadmium and citrate ions for lead as complexing agents turned out to be sensitive to IR radiation [1].

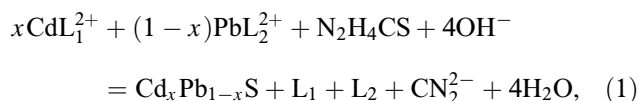
An alternative to ammonia can be ethylenediamine (NH₃)₂(CH₂)₂ (En), which, along with ammonia, has weak basic properties and will simultaneously provide an alkaline environment in the reaction bath, favorable for the decomposition of the chalcogenizer and the supply of sulfur ions S²⁻ to the reaction zone. The advantage of ethylenediamine is its lower volatility compared to an ammonia aqueous solution, which ensures the constancy of the reaction mixture pH and predictability of its effect on the kinetics of metal sulfides precipitation and, consequently, on the composition and properties of the formed solid solutions. The simultaneous use of ethylenediamine and sodium citrate for thin films chemical deposition in the CdS–PbS system is discussed by Rabinovich et al. in [13], however, the publication contains only an experimental search for the conditions of the formation of the above compounds in a rather narrow range of cadmium salt concentrations from 0.0265 to 0.03 mol/l without studying the functional properties.

Based on the results of research by the Department of Physical and Colloid Chemistry of the Ural Federal University in the field of chemical deposition of metal chalcogenides thin films, we used a scientifically based approach to create a technology for depositing semiconductor layers based on PbS and CdS and develop clear recommendations for controlling the process of their production. Its idea was, that based on the analysis of ionic equilibria created in the reaction system „Pb(CH₃COO)₂–CdCl₂–Na₃C₆H₅O₇–(NH₃)₂(CH₂)₂–N₂H₄CS“, it was possible to determine the concentration region of joint precipitation of lead and cadmium sulfides, and, consequently, the potential for the formation of solid solutions of Cd_xPb_{1-x}S [20].

Considering the above this study is devoted to the study of the morphology, elemental composition, crystalline structure, and photoelectric properties of Cd_xPb_{1-x}S solid solutions hydrochemically precipitated from reaction baths, containing citrate ions and ethylenediamine as ligands.

2. Experimental procedure

Hydrochemical deposition of films with thiourea of Cd_xPb_{1-x}S solid solutions was carried out from a reaction bath, called ethylenediamine-citrate, on preliminarily defatted ST-50-1 polycrystalline glass substrates according to the reaction



where L₁, L₂ — ligands (NH₃)₂(CH₂)₂ and C₆H₅O₇³⁻ for cadmium ions Cd²⁺ and lead Pb²⁺. Lead acetate Pb(CH₃COO)₂ (0.067 mol/l) was used as metal salts, and the cadmium chloride concentration CdCl₂ was varied within the range from 0.16 to 0.22 mol/l. Thiourea (NH₂)₂CS (0.58 mol/l) served as a supplier of sulfur ions. Citrate ions C₆H₅O₇³⁻ (0.33 mol/l) and ethylenediamine (NH₃)₂(CH₂)₂ (0.6 mol/l) played the role of ligands, and the latter additionally provided the alkaline environment necessary for hydrolytic chalcogenizer decomposition. The process of obtaining CdPbS films was carried out in a liquid thermostat „TS-TB-10“ at 353 K for 140 min. A lead sulfide film was obtained from a reaction bath of a similar composition, excluding the cadmium salt, with a process duration of 90 min.

It is known [17], that in order to compensate for the excess surface energy of the nuclei formed when stable condensation centers of the Cd_xPb_{1-x}S solid phase appear in the process of chemical deposition according to the above reaction, it is required providing a certain degree of supersaturation in sulfide of both cadmium and lead. The degree of supersaturation Δ — a value that characterizes the excess of the ionic product IP_{CdS} (IP_{PbS}) created in the reaction mixture over its solubility product SP_{CdS} (SP_{PbS}), reference value. The value of supersaturation created in the system depends on the concentration of free cadmium (lead) ions in the volume of the reaction mixture, which determines the rate of the deposition process and the features of Cd_xPb_{1-x}S solid phase formation. An analysis of the ionic equilibria created in the reaction bath used by us shows, that at cadmium chloride concentration < 0.16 mol/l, the degree of cadmium sulfide supersaturation Δ_{CdS} is 1.2 times less, than lead sulfide one Δ_{PbS}, and at > 0.22 mol/l Δ_{CdS} is 1.3 times higher than Δ_{PbS}. As a result, in the first case, only PbS is formed, and in the second case — CdS, i.e. in both cases, there are no potential conditions for the formation of a solid solution based on them.

The X-ray studies of the deposited films were carried out in the range of angles 2θ = 20–100° with an increment of 0.01° and a scanning time of 5 s at a point on a diffractometer „MiniFlex 600“ (by „Rigaku Corporation“, Japan). The refinement of the structural parameters of the Cd_xPb_{1-x}S films was carried out by the full-profile Rietveld analysis [21,22] using Fullprof [23] software.

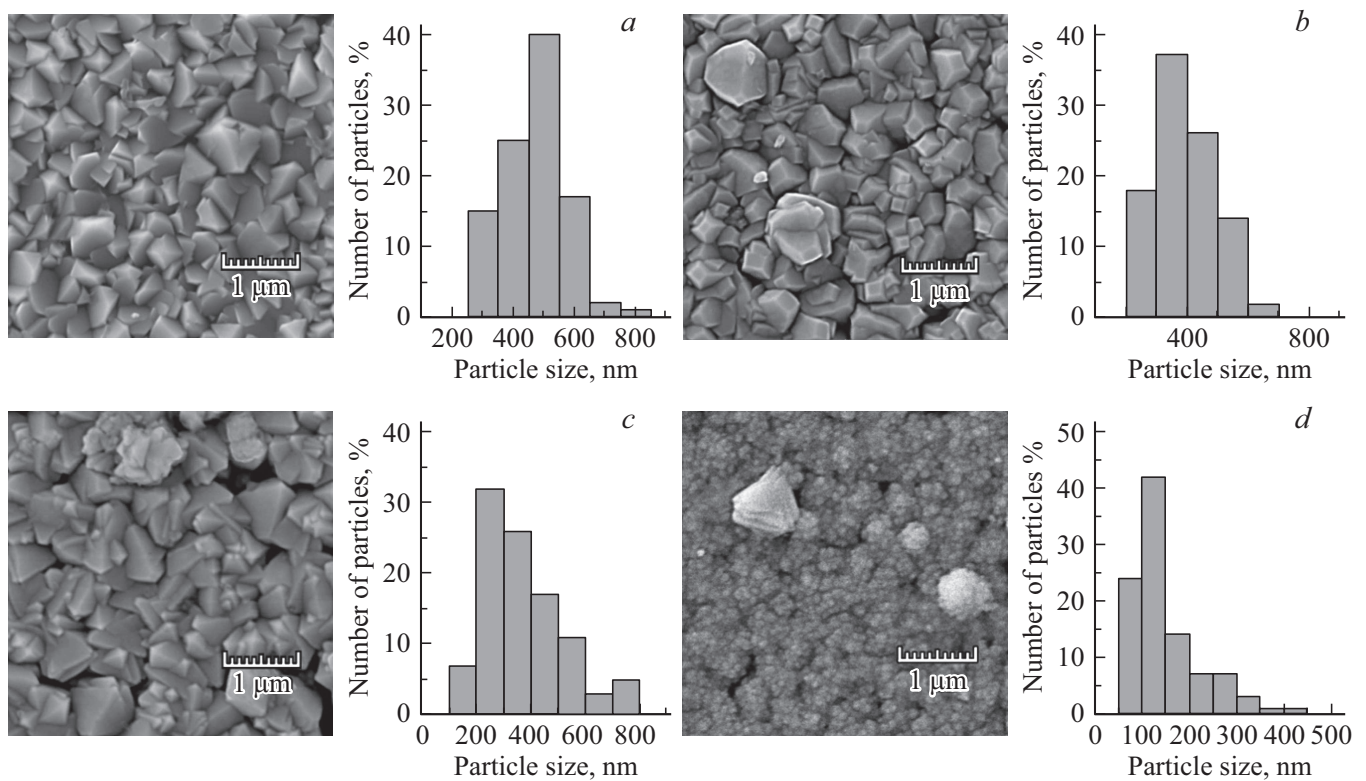


Figure 1. Electron microscopic images of CdPbS films obtained on polycrystalline glass from reaction baths containing 0.16 (a), 0.18 (b), 0.20 (c), 0.22 mol/l (d) $CdCl_2$, and particle size distribution histograms.

The morphology and elemental composition of the films were studied using scanning electron microscopes MIRA 3 LMU at an accelerating voltage of the electron beam 10 kV and JEOL JSM-5900 LV with an energy-dispersive X-ray analyzer EDS Inca Energy 250. The particle size was determined using the Measurer software with further data processing in the Grapher 9.6 application package.

To study synthesized films photoelectric properties, 20×14 mm sensor elements with electrochemically deposited nickel contacts were fabricated on the K.54.410 bench. The emission source was an absolute blackbody (ABB) with a temperature of 573 K. The effective density of the emission flux incident on the sensitive area was 10^{-4} W/cm^2 at a modulation frequency of the incident emission flux of 1000 Hz and a bias voltage of U_{bi} 100 V.

The current-voltage characteristics (CVC) of the films were recorded by the two-probe method in the applied voltage range from -10 to 10 V with a step of 100 mV at a temperature of 298 K. The current strength was determined with a Keithley 2450 source-meter. The photocurrent was recorded under illumination with a 100 mW/cm^2 light beam from a Zolix GLORIA-X500A solar radiation simulator equipped with an Osram XBO 500W/H OFR lamp.

3. Results and discussion

3.1. Morphology

The subject of research were the films of three-component CdPbS compounds, the composition of which depended on the ratio of the rates of individual lead and cadmium sulfides formation, provided by varying from 0.16 to 0.22 mol/l of cadmium chloride $CdCl_2$ in the reaction bath at fixed concentrations of the rest components. As a result, 400–650 nm layers were obtained, which have good adhesion to the substrate. The microstructure and particle-size distributions in the films under study are shown in Fig. 1.

Let us consider the evolution of the thin-film CdPbS layers morphology. In all synthesized films, a clear unimodal distribution of fairly large crystallites (300–500 nm) is observed, the proportion of which decreases, amounting to 65% (Fig. 1, a), 42% (Fig. 1, b), 25% (Fig. 1, c) and 5% with $\sim 25\%$ content of nanoparticles (Fig. 1, d).

The introduction of 0.16 mol/l cadmium salt into the reactor leads to the formation of a dense and homogeneous microstructure (Fig. 1, b), and in the presence of 0.18 mol/l $CdCl_2$ the film consists of different-sized crystallites closely adjacent to each other, representing truncated tetrahedra (Fig. 1, c). The film obtained at a content of 0.20 mol/l of cadmium chloride in the reaction bath (Fig. 1, d) contains the minimum amount of large crystallites (~ 400 – 550 nm),

on the surface of which intensive secondary nucleation of quadrangular pyramids of a smaller size (~ 100 nm) is observed. The film obtained at the maximum concentration (0.22 mol/l) differs fundamentally. It is formed from ~ 100 – 200 nm globular aggregates, which in their turn consist of nanoparticles, with inclusions of single spherical aggregates and oblate ~ 400 – 500 nm crystallites.

3.2. Crystal structure

Experimental X-ray patterns of the synthesized films of ternary CdPbS compounds are shown in Fig. 2, *a–e* and Fig. 3. The set of intense diffraction reflections from the films under discussion corresponds to a cubic face-centered lattice of NaCl type ($B1$, ex. gr. $Fm\bar{3}m$), which is typical of lead sulfide. Along with these reflections, one can see weak additional reflections, which belong to the polycrystalline glass substrate, which includes TiO_2 and cordierite $Mg_2Al_4Si_5O_{18} \cdot nH_2O$ (ex. gr. $P4/mnm$ and $Cccm(D202h)$), specified in Fig. 2 with lower dashes). Note that, apart from this set of diffraction reflections from two phases (main and substrate), no other reflections are observed in the X-ray patterns. The formation of $Cd_xPb_{1-x}S$ solid solutions with a change in the concentration of cadmium chloride in the reactor is evidenced by the gradual shift of diffraction reflections $(220)_{B1}$ to the region of larger 2θ angles (Fig. 2, *f*).

The refinement of CdPbS compounds crystalline structure parameters was carried out by the Rietveld full-profile analysis using the FullProf software, which we successfully used earlier [12]. Figures 2 and 3 show a good agreement between the experimental data and the calculation in the FullProf software, taking into account all the individual features of the structural state of the $Cd_xPb_{1-x}S$ films: NaCl-type lattice models (Fig. 2) and zinc blende (Fig. 3), lattice parameters, anisotropic broadening of reflections, preferential orientation of some grains. The calculation was carried out taking into account the presence in the X-ray pattern of additional reflections of TiO_2 titanium dioxide phase and $Mg_2Al_4Si_5O_{18} \cdot nH_2O$ cordierite, which are part of the polycrystalline glass. At the same time, it should be noted, that the software used contains an algorithm for correcting for the zero shift of the entire spectrum, deviation from the scattering plane, taking into account the angular dependence, and other corrections for instrumental errors when adjusting the sample for precision refinement of the lattice parameter. The figures show the minimal difference between the experimental (circles) and calculated (enveloping lines) X-ray patterns of CdPbS films, which confirms the high accuracy of the performed full-profile analysis.

With an increase in the concentration of cadmium chloride in the reaction bath, the reflections of the synthesized films are shifted to the region of larger angles 2θ (Fig. 2, *f*), accompanied by a monotonic decrease in the period of the cubic lattice a_{B1} in the range from 0.5918(0) to 0.5910(7) nm (Table 1). The decrease in the crystal lattice

period is due to the replacement of lead (II) ions with a radius of 0.120 nm [24] in the PbS lattice by cadmium ions with a smaller radius of 0.097 nm [25]. To estimate the content of cadmium x in the formed $Cd_xPb_{1-x}S$ solid solution, we used the crystal lattice constant of the PbS film, equal to 0.5934(3) nm, which was found earlier by us [26]. This is slightly less, than the literature value (0.5936 nm) of massive single-crystalline PbS sulfide with $B1$ (NaCl) [25] structure. To determine the relative content of cadmium in the substitutional solid solution $Cd_xPb_{1-x}S$, which retains the cubic structure of lead sulfide, it is necessary to know the lattice parameter of the CdS film. However, an X-ray study showed, that the $\sim 0.2 \mu m$ CdS film turned out to be amorphous. Therefore, for calculations we used the value of the crystalline lattice period $a_{B1} = 0.546$ nm of pseudocubic sulfide CdS, obtained in the studies [27,28]. It is known [29], that at low substitutions of lead by cadmium the dependence of the lattice parameter of the solid solution is additive $a_{SS} = f(x)$ and obeys Vegard's law [30,31]. Therefore, the estimation of the relative content of cadmium x in $Cd_xPb_{1-x}S$ was carried out using the expression $x = (a_{PbS} - a_{SS}) / (a_{PbS} - a_{CdS})$, where a_{PbS} , a_{CdS} , a_{SS} — parameters of crystalline lattices of lead, cadmium sulfides and $Cd_xPb_{1-x}S$ solid solution.

The grains formed in the films of $Cd_xPb_{1-x}S$ ($B1$) solid solutions are ordered in the $[200]$ plane direction, which is evidenced by the excess intensity of the $(200)_{B1}$ over $(111)_{B1}$. The change in the preferred grain orientation is related to the substitution of lead cations for cadmium in the initial PbS compound with (111) texture [24]. The texture of $Cd_xPb_{1-x}S$ films synthesized from reaction baths containing cadmium chloride from 0.16 to 0.19 mol/l increases from 12.2 to 17.2% (Table 1), and at 0.20 mol/l randomization of grain orientation occurs (degree of texturing $\sim 0.7\%$), which may indicate some critical concentration. The increase of grains texture $Cd_xPb_{1-x}S$ up to $\sim 38.2\%$ and the appearance of cadmium sulfide $B3$ cubic phase grains with the $(111)_{B1}$ orientation constituting 54.5%, also indicates a critical cadmium chloride concentration, equal to 0.22 mol/l.

It should be noted, that the experimental lattice cell parameters of cubic cadmium sulfide CdS (ex. gr. $F4\bar{3}m$) $a_{B3} = 0.5792$ nm are less, than the value for a single crystal $a_{B3} = 0.5818$ nm (JCPDS database, card № 10-0454). This may be due to the fact, that during the formation of this phase, due to the difference of crystalline lattices volumes of polycrystalline glass substrate and the synthesized film, the compression of the thin-film layer occurs under the action of external pressure. A similar effect of reducing the period of the lattice cell to 0.57706 and 0.57733 nm was found for thin-film CdS with the $B3$ structure obtained by chemical deposition [32].

Further the analysis of the X-ray patterns showed, that the diffraction reflections of the $Cd_xPb_{1-x}S$ solid solution films obtained from the reaction baths with 0.16–0.20 mol/l cadmium chloride are broadened (Fig. 2, *a–e*), and their broadening is anisotropic, i.e. depends on the indexes of

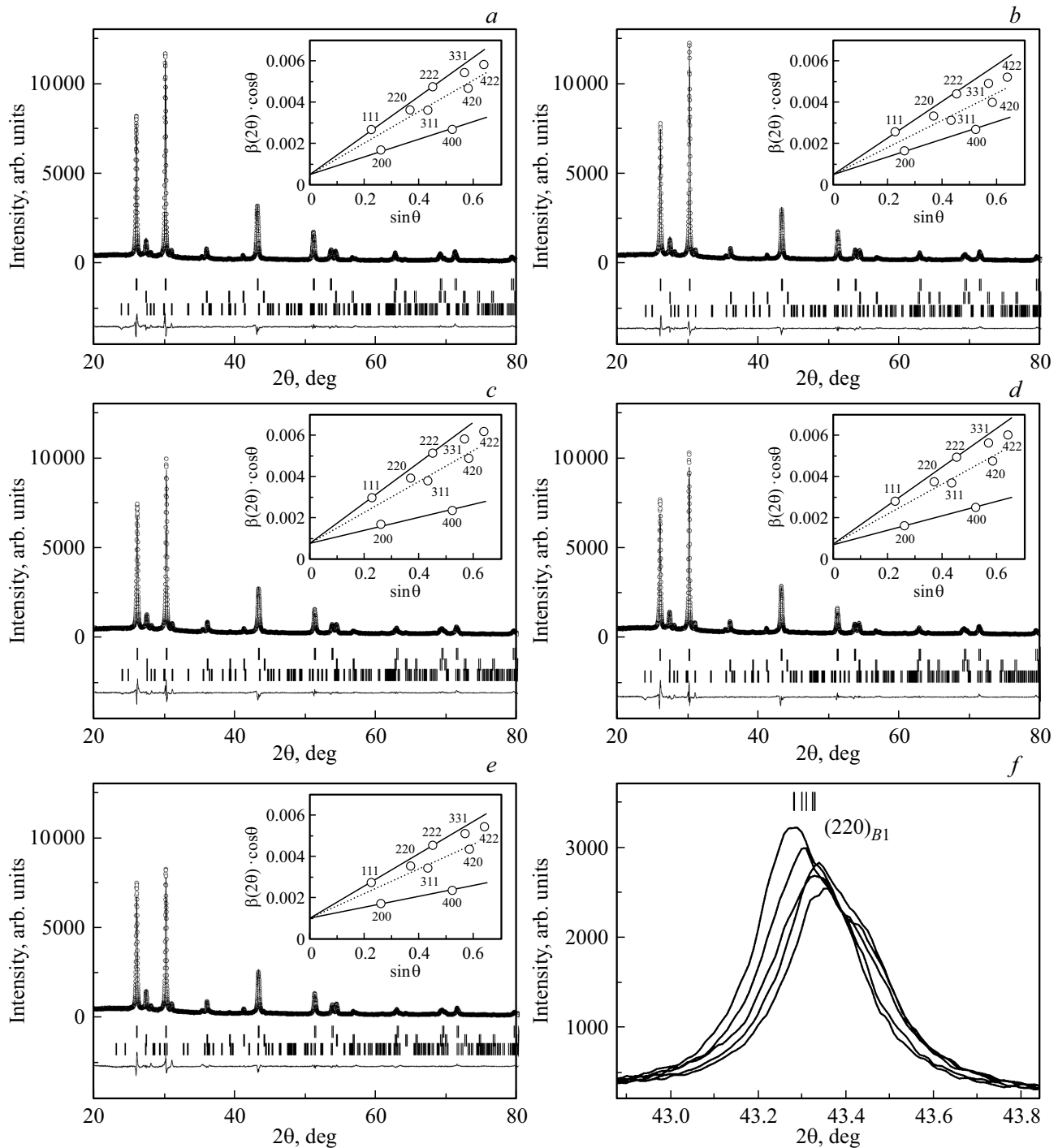


Figure 2. Experimental (circles) and calculated (enveloping lines) X-ray patterns of $Cd_xPb_{1-x}S$ solid solutions films deposited on a polycrystalline glass substrate from the reaction mixture containing 0.16 (a), 0.17 (b), 0.18 (c), 0.19 (d) and 0.20 (e) cadmium chloride. Bottom line — difference between calculation and experiment. The dashes show the angular positions of $B1$ phase reflections (upper ones), TiO_2 and the monoclinic mixture (lower ones). The inserts show the $\beta(2\theta) \cdot \cos\theta$ dependencies of $\sin\theta$. The shift of reflections of the $(220)_{B1}$ (f) face to the region of big angles 2θ .

the planes. In the general case, the broadening of the reflections is caused by two reasons: the small size of the coherent scattering regions (in the first approximation, the small size of the crystallites) and the appearance of internal microstresses in the sample. This is confirmed

by Williamson–Hall dependences $\beta \cdot (2\theta) \cdot \cos\theta$ on $\sin\theta$ shown in the inserts in Fig. 2, a–e. The inclinations of these approximating straight lines indicates the presence of microdeformations in the bulk of the film, and the cutoff segment on the ordinate axis ($\sin\theta = 0$) gives the

Table 1. The crystalline lattice parameter a_{B1} and a_{B3} , the number of grains with the predominant orientation $(200)_{B1}$ and $(111)_{B1}$ parallel to the plane of the substrate $T_{(200)}$ and $T_{(111)}$, average microdeformations $\langle \Delta d/d \rangle$, size of coherent scattering regions (D) in synthesized films

CdCl ₂ , mol/l	0.16	0.17	0.18	0.19	0.20	0.22	
						a_{B1} , nm	a_{B3} , nm
a_{B1} , nm	0.5916(7)	0.5914(4)	0.5913(1)	0.5911(3)	0.5910(7)	0.5910	0.5792
$T_{(200)}$, %	12.2	13.2	16.9	17.2	0.7	38.2	—
$T_{(111)}$, %	—	—	—	—	—	—	54.5
$\Delta d/d \cdot 10^{-4}$							
111	25.6	23.0	26.9	26.3	22.3		
200	11.1	10.2	8.1	9.6	6.9		
220	22.8	19.9	23.7	23.2	19.6		
311	19.3	15.6	19.4	19.3	16.1		
331	25.6	23.0	26.9	26.3	22.3		
400	11.1	10.2	8.1	9.6	6.9		
331	23.7	20.9	24.7	24.2	20.4		
420	19.4	15.8	19.6	19.5	16.2		
422	22.8	19.9	23.7	23.2	19.6		
$\langle \Delta d/d \rangle \cdot 10^{-4}$	20.2	19.8	20.2	20.1	16.7	19.2	28.2
D , nm	227	164	150	184	129	102	18

coherent scattering region D (in the first approximation, the grain size). Significant deviations of the experimental points from the linear dependence $\beta \cdot (2\theta) \cdot \cos\theta$ of $\sin\theta$ are observed, indicating the existence of anisotropy in thin-film layers (Table 1), due to the appearance of dislocations. At the same time, at a critical concentration in the reactor (0.22 mol/l), the microdeformations anisotropy disappears in the formed film. However, the average values $\langle \Delta d/d \rangle$ in the crystalline lattice of the studied films at cadmium chloride concentrations of 0.16–0.22 mol/l in the reactor are $(16.7–20.2) \cdot 10^4$ stay close. At the same time, a decrease in the size of the coherent scattering regions D from 227 to 102 nm is observed. In cubic CdS, one can only give estimates, assuming that the broadening is caused only by microdeformations ($\langle \Delta d/d \rangle \sim 78.2 \cdot 10^4$) or the size of coherent scattering regions (~ 18 nm).

It can be seen from the reflection intensities in Fig. 3, that CdS phase volume in the film obtained from the reaction bath in the presence of 0.22 mol/l cadmium chloride is $\sim 70–80\%$, while the volume of the solid solution $\text{Cd}_x\text{Pb}_{1-x}\text{S}$ — $30–20\%$. However, it can be seen that a strong diffuse halo from an amorphous material appeared on the X-ray pattern, most likely associated with the presence of cadmium sulfide amorphous phase. Comparison of reflection intensities in $\text{Cd}_x\text{Pb}_{1-x}\text{S}$ films (0.16–0.20 mol/l) and total reflection intensities of $\text{Cd}_x\text{Pb}_{1-x}\text{S} + \text{CdS}$ in the film obtained with 0.22 mol/l CdCl₂, allows us to say, that the volume of the crystalline phase does not exceed 10%, that correspond to the data in Table 2.

According to the estimation of the change in the lattice period, the compositions of substitutional

solid solutions obtained from reaction baths with a content of 0.16 to 0.22 mol/l CdCl₂ can be written as $\text{Cd}_{0.037}\text{Pb}_{0.963}\text{S}$, $\text{Cd}_{0.042}\text{Pb}_{0.958}\text{S}$, $\text{Cd}_{0.045}\text{Pb}_{0.955}\text{S}$, $\text{Cd}_{0.048}\text{Pb}_{0.952}\text{S}$ and $\text{Cd}_{0.050}\text{Pb}_{0.950}\text{S}$ (Table 2). Comparison of the data on the content of cadmium in layers of $\text{Cd}_x\text{Pb}_{1-x}\text{S}$ ($x \leq 0.050$) solid solutions obtained by chemi-

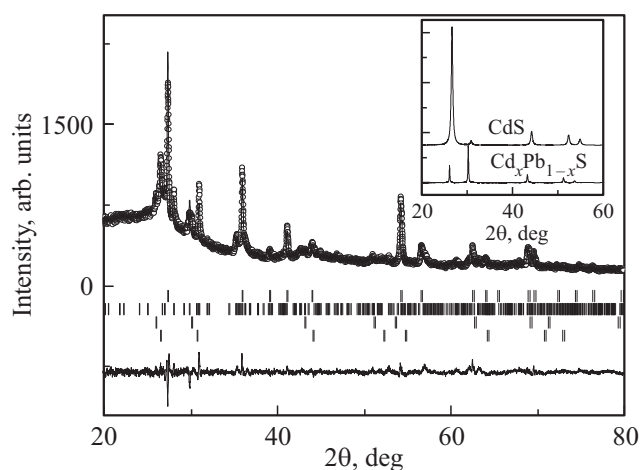


Figure 3. Experimental (circles) and calculated (enveloping lines) X-ray patterns of a CdPbS film deposited on a polycrystalline glass substrate from a reaction mixture containing 0.22 cadmium chloride. Bottom line — difference between calculation and experiment. The dashes show the angular positions of the phase reflections (2 upper rows of TiO₂ and monoclinic phase of the substrate), (2 lower rows of $\text{Cd}_x\text{Pb}_{1-x}\text{S}$ with lattice $B1$ and CdS with a cubic lattice $B3$). In the insert — X-ray patterns of CdS and PbS on the same scale, shifted along the 2θ axis for clarity.

Table 2. Effect of the $CdCl_2$ concentration in the reaction bath on the elemental composition of deposited films and the composition of $Cd_xPb_{1-x}S$ solid solutions

[$CdCl_2$], mol/l	Formular composition of $Cd_xPb_{1-x}S$ (estimation on the period of lattice)	Content of elements in film, at%			Formular composition of film (without separation into crystalline and amorphous phase)	Phase content of film, mol%	
		Cd ± 0.07	Pb ± 0.05	S ± 0.08		solid solution $Cd_xPb_{1-x}S$	amorphous CdS sulfide
0.16	$Cd_{0.037}Pb_{0.963}S$	2.02	47.77	50.21	$Cd_{0.04}Pb_{0.96}S_{1.01}$	~ 99.7	~ 0.3
0.17	$Cd_{0.042}Pb_{0.958}S$	3.04	47.17	49.79	$Cd_{0.06}Pb_{0.94}S_{0.99}$	98	2
0.18	$Cd_{0.045}Pb_{0.955}S$	3.66	46.57	49.77	$Cd_{0.07}Pb_{0.93}S_{0.99}$	97	3
0.19	$Cd_{0.048}Pb_{0.952}S$	5.09	45.25	49.66	$Cd_{0.10}Pb_{0.90}S_{0.99}$	94	6
0.20	$Cd_{0.050}Pb_{0.950}S$	5.97	44.63	49.40	$Cd_{0.12}Pb_{0.88}S_{0.98}$	93	7
0.22	$Cd_{0.050}Pb_{0.950}S$	47.59	2.84	49.57	$Cd_{0.94}Pb_{0.06}S_{0.99}$	6	94

cal precipitation at 353 K with an equilibrium phase diagram of the $CdS-PbS$ [33] system indicates a significant (three to four orders of magnitude) level of supersaturation in the substitution component.

As it is known [12], under nonequilibrium conditions of hydrochemical precipitation of lead and cadmium sulfides in an ammonia-citrate reaction bath, besides solid $Cd_xPb_{1-x}S$ substitutional solution the formation of amorphous cadmium sulfide not detected by X-ray diffraction was detected. Taking into account this fact and the morphological features of the synthesized films, it is necessary to carry out a quantitative elemental analysis.

3.3. EDX analysis

The content of the main elements (Cd, Pb, S) in freshly deposited thin-film compounds in the $CdS-PbS$ system was determined by energy-dispersive microanalysis over the entire film surface area. As it is seen from Table 2, the content of cadmium in the films under discussion significantly exceeds its content in the solid solution.

Of particular interest are the films, which differ significantly in morphology and were obtained from reaction baths containing 0.20 and 0.22 mol/l of cadmium chloride, the results of EDX analysis of which are shown in Fig. 4, and the electron microscopic image shows the regions in which the analysis was carried out. On the semiconductor layer surface obtained from the reaction bath in the presence of 0.20 mol/l cadmium chloride, single grains with an increased content of cadmium 10.08 and 21.27 at% were locally found, significantly exceeding the average value — 3.67 at%. In the second reaction bath (0.22 mol/l), a film was obtained, which included up to 47.09 at% of cadmium and only 2.84 at% of lead.

Film samples obtained from reaction baths in the presence of 0.17–0.22 mol/l $CdCl_2$ are slightly enriched in metals at the ratio (Pb + Cd):S = 1.01–1.02. In a fairly homogeneous densely packed film obtained from a bath with a cadmium chloride content of 0.16 mol/l, a small excess of chalcogen (50.21 at%) was found at a total metal content (Pb + Cd) of 47.79 at%, similar to PbS [26] film.

According to the EDX analysis and the averaged results of the energy-dispersive study, the formula composition of thin-film layers can be written as $Cd_{0.04}Pb_{0.96}S$, $Cd_{0.06}Pb_{0.94}S_{0.99}$, $Cd_{0.07}Pb_{0.93}S_{0.99}$, $Cd_{0.10}Pb_{0.90}S_{0.99}$, $Cd_{0.12}Pb_{0.88}S_{0.98}$, $Cd_{0.94}Pb_{0.06}S_{0.99}$ (Table 2).

Based on the results of research of the films under discussion, by EDX analysis and X-ray diffraction it was found, that with an increase of cadmium chloride concentration in the reactor from 0.16 to 0.20 mol/l, in addition to the substitutional solid solutions $Cd_xPb_{1-x}S$, a new phase is formed — individual cadmium sulfide CdS (Table 2). The reflections responsible for cadmium sulfide are not observed in X-ray patterns, this allows us to conclude, that CdS is in the amorphous state. Moreover, when the composition of $Cd_{0.037}Pb_{0.963}S$ solid solution obtained in the presence of 0.16 mol/l cadmium chloride in the reactor is close to the formula composition established by EDX analysis — $Cd_{0.04}Pb_{0.96}S_{1.01}$, and the proportion of the amorphous CdS phase does not exceed ~ 0.3 mol%, then with a further increase of cadmium salt concentration in the reactor, the content of individual cadmium sulfide increases to 2–7 mol%.

The redistribution of cadmium between the phases of the $Cd_xPb_{1-x}S$ solid solution and amorphous CdS can be evidenced by a sudden decrease of the layers texture from 17.2 to 0.7 and microdeformations from $20.1 \cdot 10^4$ to $16.7 \cdot 10^4$ (Table 1). Similar „transitional“ conditions under which an individual CdS phase is formed along with a solid solution were discovered by the authors using an ethylenediamine-citrate reaction mixture [13], as well as in citrate-ammonia baths [12].

At a critical concentration (0.22 mol/l $CdCl_2$), in addition to amorphous cadmium sulfide, a crystalline phase of cubic cadmium sulfide was also found; the total CdS amount reaches 94%.

A specific feature of chemical precipitation occurring in the „mild“ nonequilibrium temperature regime is the acquisition of a high Gibbs free energy, that leads to the formation of self-organizing systems that are far from equilibrium [15]. Due to the limited CdS solubility in lead

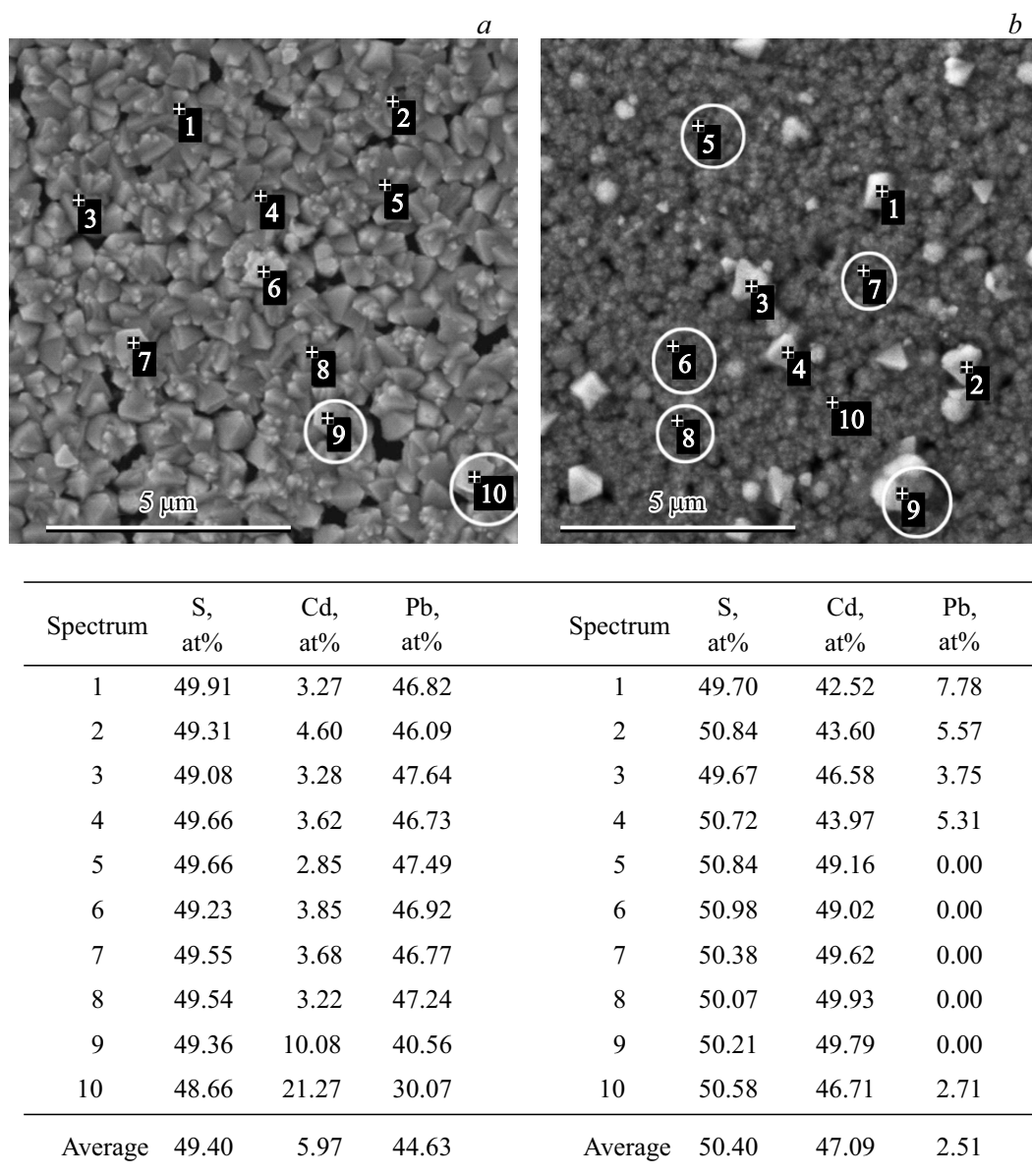


Figure 4. The results of energy-dispersive analysis of films in a system obtained by co-deposition of CdS and PbS from reaction baths containing 0.20 (a) and 0.22 mol/l (b) cadmium chloride.

sulfide, with an increase in the nonequilibrium state when cadmium salt concentration increases in the reaction bath, it becomes thermodynamically more favorable for cadmium to form its own phase, as a result, the system becomes heterophase.

The established inhomogeneity (inhomogeneity of the film sample composition), in the opinion of the authors of the study [34], can have an additional effect on the broadening of diffraction reflections. The inhomogeneity of the phase composition of semiconductor materials and crystal lattice defects directly affect the band structure, the processes of generation and recombination of charge carriers, directly determining their functional properties.

3.4. Photoelectric properties

At present, the study of the processes of optical radiation interaction with the materials under study and their relationship with the composition and structure is one of the topical problems of semiconductor materials science. Let us consider the influence of the morphology, crystal structure, elemental and phase compositions of the obtained films in the CdS–PbS system on their photoelectric properties.

The dependences of the dark resistance R_d and voltage sensitivity U_s of the resulting semiconductor layers on the concentration in the reaction cadmium chloride solution are shown in Fig. 5. The film resistance R_d increases exponentially from 2 to 80 M Ω per square with the increase of

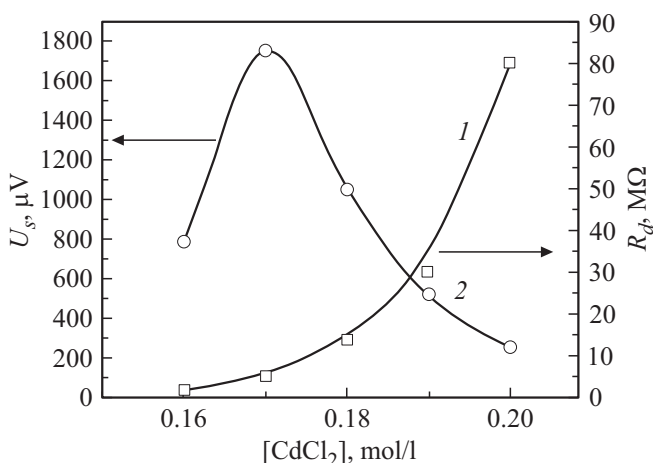


Figure 5. Dependence of dark resistance R_d (1) and voltage sensitivity U_s (2) of $Cd_xPb_{1-x}S$ on the concentration of $CdCl_2$ in the reaction mixture.

concentration $CdCl_2$ in the reaction mixture. This is due to an increase from 0.3 to 7 mol% of the amorphous CdS phase and a decrease in the average size of crystallites from ~ 500 to ~ 250 nm in the thin-film layers. Unfortunately, it was not possible to measure the voltage sensitivity and dark resistance of the film obtained from the reaction mixture in the presence of 0.22 mol/l cadmium chloride, as the film contains up to 96% of high-resistance CdS .

The synthesized layers have a relatively high sensitivity to IR radiation, while for $Cd_xPb_{1-x}S$ films synthesized from baths containing 0.16 to 0.17 mol/l $CdCl_2$, an increase in the photoresponse value is observed. The maximum value of the voltage sensitivity $1750 \mu V$ corresponds to a well-defined ratio in the thin-film layer of the solid solution $Cd_{0.042}Pb_{0.958}S$ (98%) and amorphous cadmium sulfide (2%). A further increase in the cadmium salt concentration at a fixed content

of the remaining components of the reaction bath promotes the formation of a film containing $Cd_xPb_{1-x}S$ solid solution with $x = 0.045-0.050$ and 3–7 mol% of cadmium sulfide, which is accompanied by a sudden deterioration in photosensitivity. It is known, that freshly precipitated undoped cadmium sulfide is not photosensitive [18]. However, it should be noted that, probably, there is a certain threshold amount of the amorphous CdS phase, the excess of which is accompanied by a decrease in photosensitivity, as we found earlier in the chemical deposition of films in the $CdS-PbS$ system from ammonia-citrate reaction baths in the presence of cadmium acetate [35]. In the films from this reaction bath, the limiting content of high-resistivity cadmium sulfide was much higher and amounted to ~ 26 mol%. A comparison of these data allows us to conclude, that the maximum value of the photoresponse corresponds to a certain ratio of the crystalline and amorphous phases in the layers, the content of which depends both on the complexing agents used and on the nature of the anionic component of the cadmium salt.

An analysis of the literature data shows, that photovoltaic films have a very complex internal structural structure; they obviously consist of various block asymmetric micropotential barriers, i.e. a heterojunction [36] is formed.

In our case, a heterojunction can be formed in synthesized films containing a $Cd_xPb_{1-x}S$ ($0.042 \geq x \leq 0.05$) solid solution conductivity p -type and CdS n -type. In this connection, the current-voltage characteristics of the synthesized films were studied, which have a linear form over the entire range of applied voltages (Fig. 6, a). Consequently, the current transfer through the synthesized layers obeys Ohm's law. The increase in current strength after illumination of the surface of the studied films is due to the generation of additional electron-hole pairs excited by the incident light. At the same time, in the synthesized layers, the photocurrent increased by $\sim 2.4, 10.7, 24.5, 27.1$ and 56 times compared to the dark current I_l/I_d , which

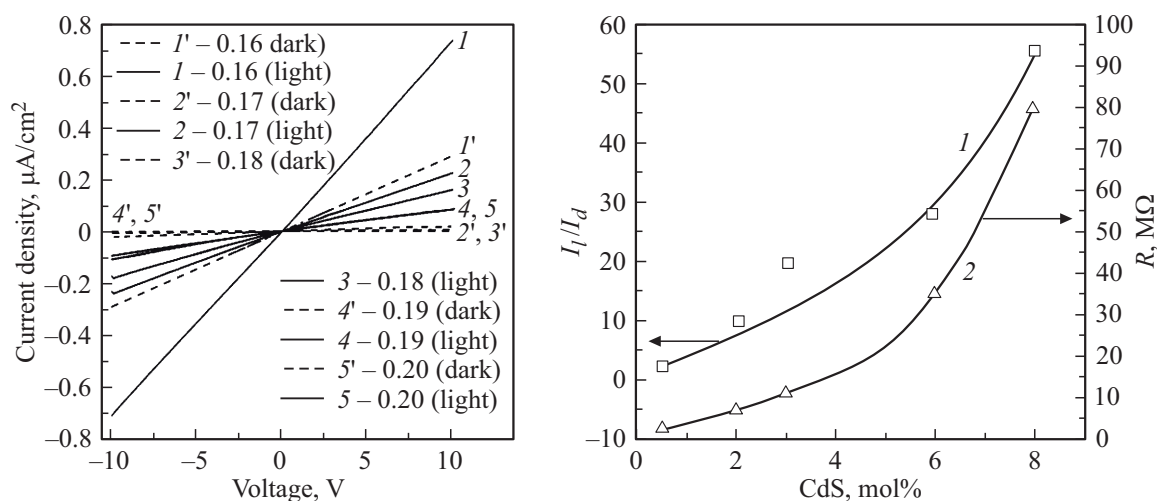


Figure 6. Current-voltage of films ($Cd_xPb_{1-x}S + CdS$) depending on the concentration of cadmium chloride in the reaction bath (a). Dependence of the ratio of light and dark currents I_l/I_d (1), as well as the dark resistance R_d (2) of the layer on the content of the amorphous CdS phase in the films ($Cd_xPb_{1-x}S + CdS$) (b).

is probably due to an increase of CdS content from 0.3 to 7 mol% in the synthesized films in addition to the $\text{Cd}_x\text{Pb}_{1-x}\text{S}$ solid solution (Fig. 6, b).

At interfacial contact, for example, a $\text{Cd}_x\text{Pb}_{1-x}\text{S}$ solid solution and amorphous CdS, a potential barrier and a space charge region are formed. When the barrier structure is illuminated, charge carriers are generated, followed by the separation with barrier electric field. If the illuminated diode structure is closed to external resistance, then a current appears in the circuit. Consequently, it is expedient to associate the photoelectric properties of two-phase $\text{Cd}_x\text{Pb}_{1-x}\text{S} + \text{CdS}$ films with the formation of potential barriers at the boundaries of crystal grains.

The mechanism of photoconductivity of thin PbS films and $\text{Cd}_x\text{Pb}_{1-x}\text{S}$ solid solutions has not been fully established. The following model was proposed in [37]: there are inversion layers on the surface of PbS particles in intercrystalline interlayers, the existence of which is due to the presence of impurity phases and having a different type of conductivity. As a result, an inversion channel is formed, in which the charge carriers transport occurs and current is transferred. Since cadmium sulfide has electronic conductivity [38], and the semiconductor layers synthesized by us have an acceptor layer, nanoparticles of the individual CdS phase can act as such inversion layers. When the film is illuminated by a light beam of 100 mW/cm^2 , the electrons and holes generated in the bulk of the crystallites are separated in space upon diffusion to the crystallites surface. Spatial separation prevents the recombination of photoholes and photoelectrons; therefore, their lifetime increases significantly in comparison with the bulk one, and the photocurrent also increases. Thus, CdS nanoparticles can play an important role in the implementation of the photoconductivity mechanism in the layers under discussion.

However, there is a limiting value for the thickness of such a „channel“, when diffusing electrons begin to recombine with CdS particles structure holes, the source of which are lattice defects. The resistance of the semiconductor layer increases, and the photosensitivity decreases.

4. Conclusion

By joint chemical precipitation of PbS and CdS sulfides from an ethylenediamine-citrate reaction mixture when varying the CdCl_2 salt concentration from 0.16 to 0.22 mol/l, thin films of three-component CdPbS compounds with good adhesion to polycrystalline glass substrate were obtained. X-ray diffraction revealed the formation of supersaturated substitutional solid solutions $\text{Cd}_x\text{Pb}_{1-x}\text{S}$ ($0 < x \leq 0.05$) with a cubic structure $B1$ (space group $Fm\bar{3}m$), as well as amorphous cadmium sulfide. When the content of CdCl_2 reaches 0.22 mol/l, along with polycrystalline $\text{Cd}_x\text{Pb}_{1-x}\text{S}$ ($x = 0.05$), CdS crystalline phase with a cubic structure $B3$ (space group $F4\bar{3}m$) is formed. Using full-profile analysis of X-ray patterns and computer simulation in the FullProf their

structural characteristics (texturing, microdeformations, coherent scattering region) were calculated. By means of EDX analysis the excess of the cadmium content in the synthesized films compared to its amount estimated by X-ray diffraction, associated with the formation from 0.3 to 7 mol% of amorphous CdS was found. It is shown that an increase in the concentration of cadmium chloride in the reaction bath to a certain critical concentration (0.22 mol/l) generates a directed macroscopic process of the formation of a crystalline phase of cadmium sulfide with a content of up to 94 mol% in the layer.

The extreme nature of the dependence of the voltage sensitivity with an increase in the concentration of cadmium chloride in the reaction bath is associated with the achievement of a certain ratio of the solid solution $\text{Cd}_{0.042}\text{Pb}_{0.958}\text{S}$ (98%) and amorphous cadmium sulfide (2%) in a thin film layer. In this case, with an increase in the amorphous cadmium sulfide phase, the dark resistance of the films increases monotonically from 2 to $80 \text{ M}\Omega$ per square.

Irradiation with a light flux of 100 mW/cm^2 provides an increase in the ratio I_l/I_d in the synthesized films by $\sim 2.4\text{--}5.6$ times, which correlates with an increase in the content of the amorphous CdS phase in them from 0.3 to 7 mol%. An assumption is made about the possibility of formation of $\text{CdS/Cd}_x\text{Pb}_{1-x}\text{S}$ heterostructures in films.

Funding

This study was supported financially by the grant RFBR 20-48-660041p_a and the state assignment of the Ministry of Science and Higher Education of the Russian Federation (subject No. H687.42B.223/20, subject „Flux“ No. AAAA-A18-118020190112-8).

Conflict of interest

The authors declare that they have no conflict of interest.

References

- [1] L.N. Maskaeva, V.F. Markov, M.Yu. Porhachev, O.A. Mokrousova. *Pozharovzryvobezopasnost*, **24** (9), 67 (2015).
- [2] E. Pentia, V. Draghici, G. Sarau, B. Mereu, L. Pintilie, F. Sava, M. Popescu. *J. Electrochem. Soc.*, **151** (11), G729 (2004).
- [3] A. Ounissi, N. Ouddai, S. Achour. *EPJ. Appl. Phys.*, **37** (3), 241 (2007).
- [4] B. Touati, A. Gassoumi, C. Guasch, N.K. Turki. *Mater. Sci. Semicond. Proc.*, **67**, 20 (2017).
- [5] G.H.T. Au, W.Y. Shih, S.-J. Tseng, W.-H. Shih. *Nanotech.*, **23**, 275601 (2012).
- [6] G.-L. Tan, L. Liu, W. Wgu. *AIP Advances*, **4**(6), 067107 (2014).
- [7] P.L. Nichols, Z. Liu, L. Yin, S. Turkdogan, F. Fan, C.Z. Ning. *Nano Lett.*, **15** (2), 909 (2015).
- [8] E.M. Nasir, I.S. Naji. *Aust. J. Basic & Appl. Sci.*, **9** (20), 364 (2015).
- [9] C. Rajashree, A.R. Balu, V.S. Nagarethinam. *Surf. Eng.*, **31** (4), 316 (2015).

- [10] M. Kamruzzaman, R. Dutta, J. Podder. *Semiconductors*, **46** (7), 957 (2012).
- [11] A.R. Patil. *JETIR*, **6** (3), 570 (2019).
- [12] L.N. Maskaeva, E.V. Mostovshchikova, I.V. Vaganova, V.F. Markov, V.I. Voronin, A.D. Kutyavina, I.N. Miroshnikova, E.G. Vovkotrub. *Thin Sol. Films*, **718**, 138468 (2021).
- [13] E. Rabinovich, E. Wachtel, G. Hodes. *Thin Sol. Films*, **517** (2), 737 (2008).
- [14] M. Barote, A. Yadav, E. Masumdar. *Chalcogenide Lett.*, **8** (2), 129 (2011).
- [15] L.N. Maskaeva, A.D. Kutyavina, V.F. Markov, I.V. Vaganova, V.I. Voronin. *ZhOKh*, **88** (2), 319 (2018) (in Russian).
- [16] M.A. Barote, S.S. Kamble, L.P. Deshmukh, E.U. Masumdar. *Ceram. Int.*, **39**, 1463 (2013).
- [17] V.F. Markov, L.N. Maskaeva, P.N. Ivanov. *Gidrohimiches-koe osazhdenie plenok sulfidov metallov: modelirovanie, eksperiment* (Ekaterinburg, UrO RAN, 2006) (in Russian).
- [18] V. Rakovics. *MRS Proceedings*, **900E**, (2005).
- [19] K.E. Suryavanshi, R.B. Dhake, A.M. Patil, M.R. Sonawane. *Optik*, **218**, 165008 (2020).
- [20] N.A. Forostyanaya, L.N. Maskaeva, A.D. Kutyavina, M.A. Ponomareva, A.A. Rozhina, P.O. Mihnevich, V.F. Markov. *Butlerovskie soobshcheniya*, **46** (5), 80 (2016) (in Russian).
- [21] H.M. Rietveld. *J. Appl. Crystallogr.*, **2** (2), 65 (1969).
- [22] D.L. Bush, J.E. Post. *Rev. Miner.*, **20**, 369 (1990).
- [23] J. Rodrigues-Carvajal. *Physica B*, **192** (1–2), 55 (1993).
- [24] L.T. Bugaenko, S.M. Ryabih, A.L. Bugaenko. *Vestn. MGU. Ser. 2. Khimiya*, **49** (6), 363 (2008) (in Russian).
- [25] M. Lach-hab, D.A. Papaconstantopoulos, M.J. Mehl. *J. Phys. Chem. Solids*, **63**, 833 (2002).
- [26] A.D. Kutyavina, L.N. Maskaeva, V.I. Voronin, I.A. Anokhina, V.F. Markov. *CTA*, **8** (2), 20218210 (2021).
- [27] J.A. Corll. *J. Appl. Phys.*, **35** (10), 3032 (1964).
- [28] K. Susa, T. Kobayashi, S. Taniguchi. *Solid State Chem.*, **33**, 197 (1980).
- [29] A.V. Chichagov, L.V. Sipavina. *Parametry yacheek tverdyh rastvorov* (M., Nauka, 1982) (in Russian).
- [30] L. Vegard. *Zeitschrift Phys.*, **5**, 17 (1921).
- [31] A.R. Denton, N.W. Ashcroft. *Phys. Rev. A*, **43**, 3161 (1991).
- [32] R. Lozada-Morales, O. Zelaya-Angel. *Cryst. Res. Technol.*, **39** (12), 1115 (2004).
- [33] L.E. Shelimova, V.N. Tomashik V.I. Gricyv. *Diagrammy sostoyaniya v poluprovodnikovom materialovedenii (sistemy na osnove hal'kogenidov Si, Ge, Sn, Pb)* (M., Nauka, 1991) (in Russian).
- [34] A.S. Kurlov, A.I. Gusev. *Fizika i khimiya stekla*, **33** (3), 383 (2007) (in Russian).
- [35] L.N. Maskaeva, I.V. Vaganova, V.F. Markov, A.E. Bezdetnova, A.D. Selyanina, V.I. Voronin, I.O. Selyanin. *FTP*, **55** (12), 1186 (2021) (in Russian).
- [36] H.M. Sulajmonov, H.T. Juldashv, O.R. Nurmatov, T.I. Rahmonov, H.E. Muhammadyakubov. *Izv. Oshckogo tekhnologicheskogo un-ta*, **3**, 180 (2019) (in Russian).
- [37] L.N. Neustroev, V.V. Osipov. *FTP*, **20** (1), 59 (1986) (in Russian).
- [38] R.Y. Petrus, H.A. Ilchuk, A.I. Kashuba, I.V. Semkiv, E.O. Zmiiovskaya. *JAS*, **126** (3), 220 (2019).